Application of Elliptical Properties in Building a Tomographic Image of an Inspected Object Using Multi-Element Ultrasonic Sensor Data

Yuliya Shulgina, Evgeny Shulgin, Ahmed Abouellail, Mariya Kostina, Oksana Terentyeva, and Jianglei Chang

Abstract The article discusses a proposed method that allows to reduce the amount of transmitted data from the receiving and data preprocessing to a personal computer, as well as the amount of digitized information and the time of its processing. The method is based on the main property of the ellipse. The developed data processing algorithm for a system with a multi-element sensor was tested in the MatLab software package. A block diagram and data processing algorithm have been developed for practical implementation on FPGAs. The amount of digitized information has been reduced by more than 10 times.

Y. Shulgina · E. Shulgin · A. Abouellail · M. Kostina (✉) · O. Terentyeva · J. Chang
Division for Electronic Engineering, School of Non-Destructive Testing, National Research Tomsk Polytechnic University, 30 Lenin Avenue, Tomsk, Russia 634050
e-mail: mashenkasoldatova@mail.ru

Y. Shulgina
e-mail: shulgina@tpu.ru

E. Shulgin
e-mail: sembox@mail.ru

A. Abouellail
e-mail: demo092@tpu.ru

O. Terentyeva
e-mail: oksanaterenteva95@mail.ru

J. Chang
e-mail: vastchan@mail.ru

M. Kostina
Department of Innovation Management, Tomsk State University of Control Systems and Radioelectronics, 40 Lenin Avenue, Tomsk, Russia 634050

I. V. Minin et al. (eds.), *Progress in Material Science and Engineering*,
Studies in Systems, Decision and Control 351,
https://doi.org/10.1007/978-3-030-68103-6_2

1 Introduction

Currently, ultrasonic non-destructive testing has entered a new stage of development. The possibility of obtaining a three-dimensional image of the test object with a high scanning speed in real time has been developed due to the use of multi-element sensors. Recently, the sampling phased array method (SPA), developed at the Fraunhofer Institute of nondestructive testing in Germany, is actively used to solve many problems of nondestructive testing. The essence of this method is the alternate excitation of the elements that make up the sensor, and the parallel reception of signals by all elements. The received ultrasonic signals are stored for each element of the phased array and serve as the initial data for 2D and 3D visualization of the test object. Thus, even after one cycle of transmission and reception, all angles of propagation of ultrasonic signals over the entire probing depth can be carried out, which will make it possible to reproduce the image of the object under study. Since the focusing of the ultrasonic beam is carried out not physically, but during the processing of the received data, a high scanning speed can be achieved.

The complexity of the development of devices containing multi-element sensors involves the need to transfer and process a large amount of data. Therefore, reducing the amount of recorded and transmitted information is an urgent task. With the increase in the number of the antenna array elements, the system becomes more complex and the amount of transmitted information increases. Conversion of an analog signal from an acoustic sensor into a digital sequence with a different sampling clock cycle can significantly reduce the amount of information transmitted to a personal computer or display device, as well as reduce the processing time.

2 The Principle of Constructing an Image of the Tested Object

The scanned area of the test object, located under the phased antenna array, is determined by the distance between adjacent radiating elements, the radiation pattern of the array and the frequency of the ultrasonic signal.

At the first step of the device operation, the first emitter is excited (Fig. 1), after which all elements of the array begin to receive the reflected signal [1, 2]. The received signals are fed through an amplifier to an analog-to-digital converter (ADC). The ADC, in the classic method, operates at a constant frequency clock. In this case, as will be shown below, the device memory is filled with information, some of which will not participate in image reconstruction. At the second step, the second element of the sensor is excited, after which all elements of the array receive the reflected signals. This procedure continues until all the elements of the array have been iterated over. In this case, with the increase in the number of elements in the acoustic array [3], the amount of digitized information increases in proportion to the square of their quantity.

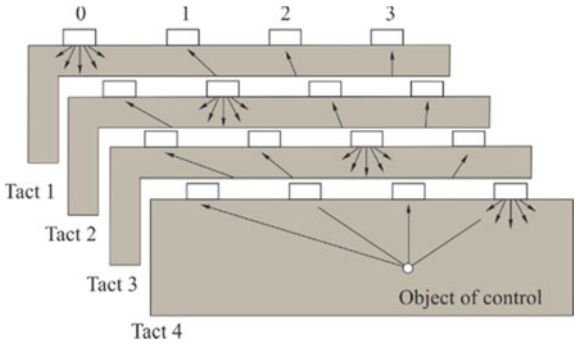

Fig. 1 The operational cycle of a 4 element sensor

To scan the area under the sensors, only four cycles of ultrasound "transmission-reception" are required for a phased array consisting of four elements, which increases the scanning speed compared to focusing the beams at each point of the tested object.

The recorded signal amplitudes at discrete times of A-scans for all emitter-receiver combinations are used in imaging. According to the calculated propagation time of the signal to the current calculated point of the tested object, the required amplitudes are sampled from each A-scan. The amplitudes for a point from all A-scans are summed together and interpreted as an image.

It is more convenient to set the point of the inspected object N by its x–y coordinates. To process one of the recorded A-scans, with the help of the emitter number N_e and the receiver number N_r, the ultrasound propagation time from the emitter to the receiver through the calculated point is calculated [4–7].

$$t_{N(x,y)\sum} = t_{ERN(x,y)} + t_{REN(x,y)}; \tag{1}$$

where $t_{ERN(x,y)}$—propagation time of ultrasound from the emitter to the point j; $t_{REN(x,y)}$—propagation time of ultrasound from point j to the receiver.

For the classical implementation of the SPA method, all distances calculated from each sensor to each point and from each point to each receiver are (Fig. 2). As a result, there is a table that contains information about the distances traveled by the ultrasound, depending on the point number, the number of the emitting sensor and the number of the receiving sensor [8]. Such a matrix will have the form shown in Table 1. In fact, there is a three-dimensional matrix for physical storage, but a two-dimensional matrix is used in this case, where the numbers of receivers and emitters are encoded by one variable.

The high demand for information processing speed leads to the necessity to perform a large number of operations simultaneously [9]. Either several high-performance processes for solving problems in parallel, or using programmable matrices, can allow for a large number of operations to be carried out in parallel on one chip.

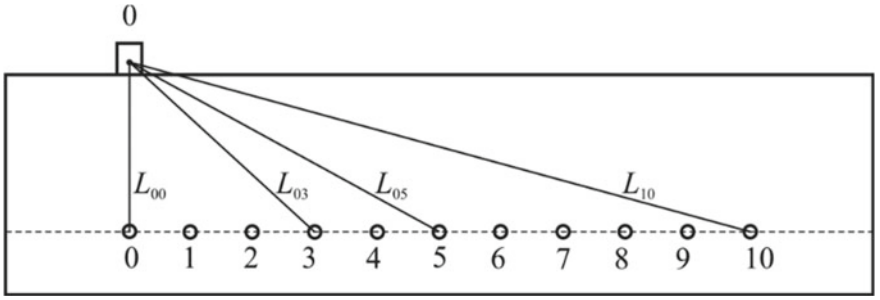

Fig. 2 Determination of the distance traveled by the signal from the source to the receiver through the calculated point

For the formation of a tomographic image of the tested object, a long post-processing time is required, because of the large number of distances determinations of signal reception and transmission by piezoelectric transducers through each digital focal point of the unltasonic signal. For example, to construct a tomographic image of the internal structure of a tested object with a size of 100 × 100 focal points of the ultrasonic signal and using an antenna array of 16 piezoelectric transducers, it is necessary to determine 2,560,000 distances.

To build an image of the tested object, it is necessary to calculate the resulting matrix, in rows and columns of which the total values of the amplitudes at a given point will be located [10–13].

The dimension of the matrix designed to store the resulting amplitude for each given point of the tested object coincides with the dimension of the image of the tested object. Therefore, with an increase in the resolution of the inspected area, the amount of stored and transmitted information increases proportionally.

3 Application of Ellipse Properties in Processing, Storing and Transmitting Information of a Tested Object

To implement the proposed processing algorithm, it is necessary to divide the scanned area of the tested object into separate scan points, as shown in Fig. 3. In this case, the same number of scanned points must be placed between adjacent sensors [14].

The essence of shortening the matrix is that the ultrasonic signal propagates radially, therefore, for any pair of emitter/receiver, there will be a set of points located at the same distances. These points will lie on the ellipse, as shown in Fig. 4. In this case, the selected transmitter and receiver will be in the focus of the ellipse. The distance between the selected emitter and receiver will determine the focal distance. The semi-minor axis of the ellipse will determine the probing depth [15].

Table 1 Complete matrix of distances for 10 points and three transmitters and receivers

Point No	Emitter 0 Receiver 0	Emitter 0 Receiver 1	Emitter 0 Receiver 2	Emitter 1 Receiver 0	Emitter 1 Receiver 1	Emitter 1 Receiver 2	Emitter 2 Receiver 0	Emitter 2 Receiver 1	Emitter 2 Receiver 2
0	L_{00}	L_{05}	L_{10}	L_{00}	L_{05}	L_{10}	L_{00}	L_{05}	L_{10}
1	L_{01}	L_{04}	L_{09}	L_{01}	L_{04}	L_{09}	L_{01}	L_{04}	L_{09}
2	L_{02}	L_{03}	L_{08}	L_{02}	L_{03}	L_{08}	L_{02}	L_{03}	L_{08}
3	L_{03}	L_{02}	L_{07}	L_{03}	L_{02}	L_{07}	L_{03}	L_{02}	L_{07}
4	L_{04}	L_{01}	L_{06}	L_{04}	L_{01}	L_{06}	L_{04}	L_{01}	L_{06}
5	L_{05}	L_{00}	L_{05}	L_{05}	L_{00}	L_{05}	L_{05}	L_{00}	L_{05}
6	L_{06}	L_{01}	L_{04}	L_{06}	L_{01}	L_{04}	L_{06}	L_{01}	L_{04}
7	L_{07}	L_{02}	L_{03}	L_{07}	L_{02}	L_{03}	L_{07}	L_{02}	L_{03}
8	L_{08}	L_{03}	L_{02}	L_{08}	L_{03}	L_{02}	L_{08}	L_{03}	L_{02}
9	L_{09}	L_{04}	L_{01}	L_{09}	L_{04}	L_{01}	L_{09}	L_{04}	L_{01}
10	L_{10}	L_{05}	L_{00}	L_{10}	L_{05}	L_{00}	L_{10}	L_{05}	L_{00}

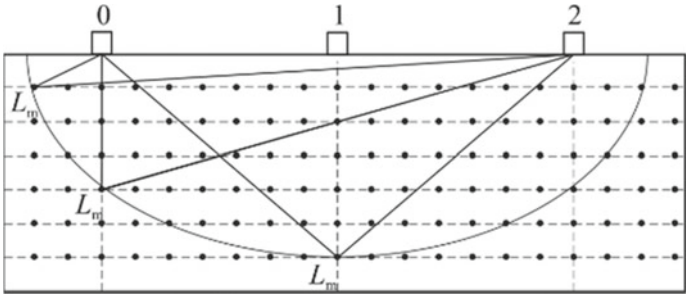

Fig. 3 The location of the pixels in the testing aria

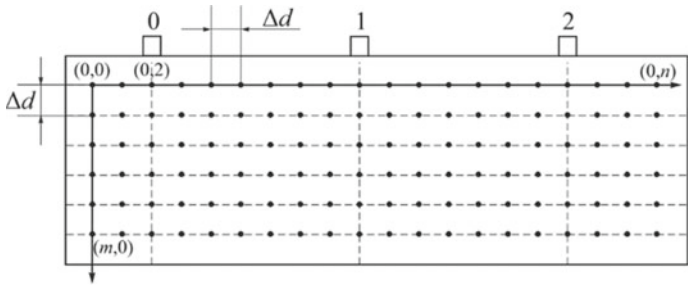

Fig. 4 Sample capture of pixels in the testing aria by using the ellipse method

It is possible to store information about the signal amplitude only for points that are a small radius of the ellipse (Fig. 5). In this case, it is possible to carry out analog-to-digital conversion of the received signal only at fixed points in time corresponding to a distance equal to the minor axis (Fig. 6).

Equally spaced points for a given combination of emitter and receiver lie on the line of the ellipse, therefore, by dividing the image of the tested object not into points, but rather into sectors of the ellipse, it is possible to sample the amplitudes from the

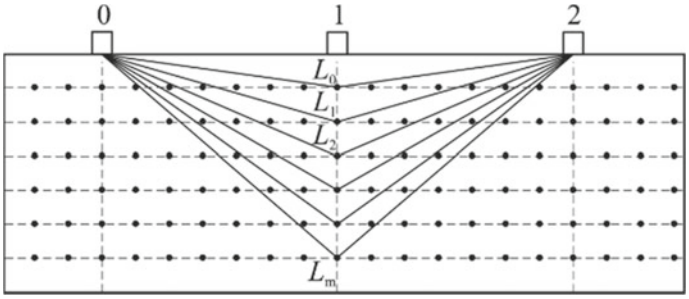

Fig. 5 Sample capture of pixels located on a small radius of an ellipse

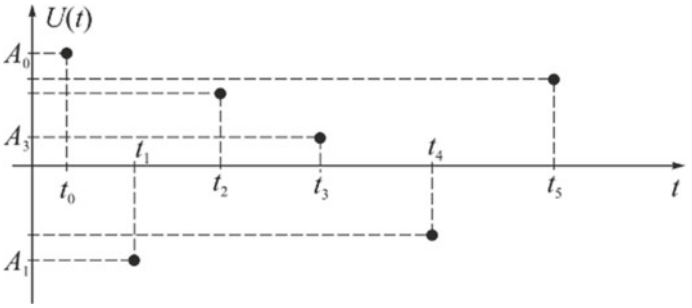

Fig. 6 An example of sample capture amplitudes of pixels located on a small radius of an ellipse

Table 2 Abbreviated matrix of distances (times) by the method of ellipses

Point number	Distance
0	L_0
1	L_1
2	L_2
3	L_3
4	L_4
5	L_5
…	…
m	L_m

A-scan memory only for points that are at an equal distance from the centers of the ellipse [16, 17].

As a result, we will have a matrix-column (Table 2), which will be completed to a complete picture of the tested object in the image processing unit.

For the data storage system, the use of the ellipse properties is very convenient, as the load on the transmitting channel is also reduced by a large factor. However, it is required to develop an imaging unit that implements an algorithm for calculating the coordinates of points located on the ellipse line.

The main difficulty in implementing the described method involves organizing the ADC clock, which requires calculating the time coordinates of the next sample and initializing the clock signal at the right time.

The clock generator, connected to the analog-to-digital conversion start unit, sets the frequency of the circuit. However, the use of programmable logic integrated circuits allows these calculations to be carried out in parallel with the recording and processing of the acoustic signal, which will make it possible to implement a system for constructing an image of the tested object in real time [18, 19].

4 Results of the Implementation of Ellipse Properties

Real signals from the antenna array were used to debug the data processing algorithm and build the image. For information processing and image construction, MATLAB programming and mathematical modeling package was selected.

The algorithm for obtaining an image using the MATLAB package is as follows (Fig. 7).

For each emitter-receiver pair, the propagation time of the ultrasonic pulse from the emitter to the receiver through the calculated point of the tested object, located on the minor axis of the ellipse, is calculated and summed.

Based on the calculated time, a column matrix is formed that stores information about the signal amplitudes at points located on the minor axis of the ellipse corresponding to the calculated row [20].

The next step is to form the image matrix, which is filled with the amplitude values by the points located on the ellipse.

After receiving image matrices from all pairs of sensors, they are summed up. The resulting matrix is displayed as an image using the images function.

Plexiglas was used as an object of control. The main data for the construction of the image was the distance between the sensors (0.75 mm), the sampling frequency (40 MHz), the ultrasound speed (2800 m/s), the number of sensors (16).

As a result of information processing in the MATLAB environment, a cross-sectional image of the examined object was built.

5 Experiment

Plexiglas with internal defects was used as an object of inspection and information was taken from a grid consisting of 16 elements, where the distance between the 16 sensors is 0.75 mm, the sampling frequency is 40 MHz, and the ultrasound speed is 2800 m/s. After one cycle of operation of the multielement sensor, 512 A-scans are obtained: 256 A-scans with constant sampling time (16 MHz) and 256 A-scans with variable sampling time.

The data was processed in two ways: the classical method and the ellipse method. Comparison of the two results was performed numerically and visually. When the imaging zone was limited by the main lobe of the sensor directional pattern, the discrepancies were observed only on the sides and amounted to less than 5%. Visually, the images obtained by the two methods did not differ. The results were visualized in the MathLab software package.

The resulting cross-sectional image of the examined object (Fig. 8) completely coincides with the image obtained using the existing algorithm, which confirms the adequacy and applicability of the developed method.

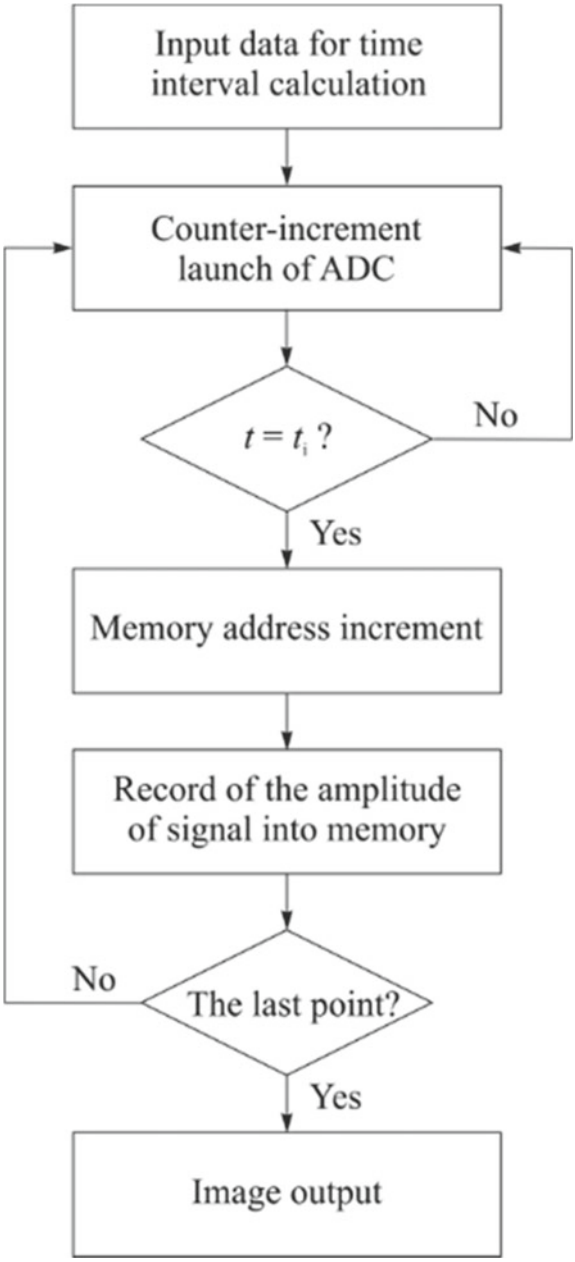

Fig. 7 Algorithm of the program in MatLab

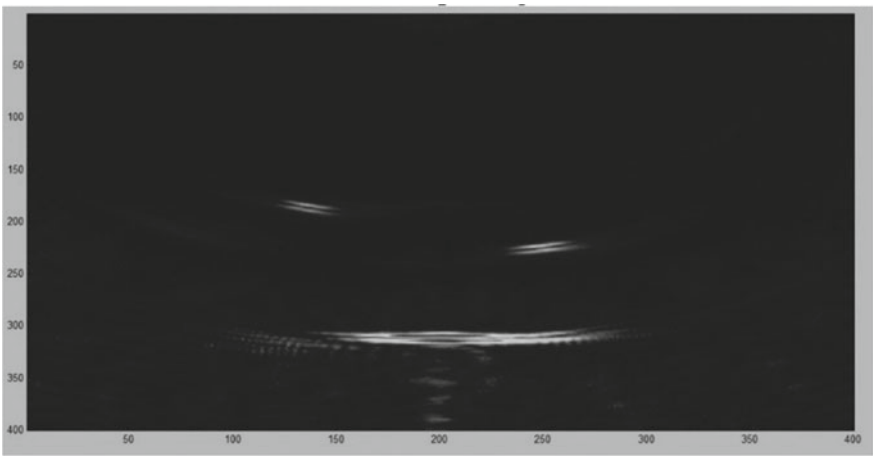

Fig. 8 Cross-sectional image of the examined object

6 Conclusion

The number of A-scan points significantly influences the processing time. When using the classical method for the object under study (plexiglass), 7818 A-scan points are required in order to satisfy all angles of the acoustic signal propagation for the selected resolution. However, when using the ellipse method, only 500 A-scan points are required, which means that the memory size for storing one A-scan will decrease 15.5 times.

The number of clock cycles per ADC cycle when processing one A-scan using the ellipse method has decreased 15.5 times, therefore, ADCs can be used operating at a lower frequency without losing image quality.

This significantly reduces the information that will be transmitted to the display system or the connected computer. The load on the information channel with the implementation of preprocessing in the programmable logic matrix will decrease by N^2 times, where N is the number of emitters in the sensor.

References

1. Bazulin, E.G., Sadykov, M.S.: Determining the speed of longitudinal waves in an isotropic homogeneous welded joint using echo signals measured by two antenna arrays. Russ. J. Nondestruct. Test. **54**(5), 303–315 (2018). https://doi.org/10.1134/S1061830918050029
2. Bazulin, E.G.: Allowing for inhomogeneous anisotropy of a welded joint when reconstructing reflector images from echo signals received by an ultrasonic antenna array. Russ. J. Nondestruct. Test. **53**(1), 9–22 (2017). https://doi.org/10.1134/S1061830917010028
3. Le Jeune, L., Robert, S., Lopez Villaverde, E., Prada, C.: Wave Imaging for ultrasonic non-destructive testing: Generalization to multimodal imaging. Ultrasonics **64**, 128–138 (2016).

https://doi.org/10.1016/j.ultras.2015.08.008
4. Camacho, J., Atehortua, D., Cruza, J.F., Brizuela, J., Ealo, J.: Ultrasonic crack evaluation by phase coherence processing and TFM and its application to online monitoring in fatigue tests. NDT E Int. **93**, 164–174 (2018). https://doi.org/10.1016/j.ndteint.2017.10.007
5. Brath, A.J., Simonetti, F.: Phased array imaging of complex-geometry composite components. IEEE Trans. Ultrason. Ferroelectr. Freq. Control **64**(10), 1573–1582 (2017). https://doi.org/10.1109/TUFFC.2017.2726819
6. Malkin, R.E., Franklin, A.C., Bevan, R.L., Kikura, H., Drinkwater, B.W.: Surface reconstruction accuracy using ultrasonic arrays: application to non-destructive testing. NDT E Int. **96**, 26–34 (2018). https://doi.org/10.1016/j.ndteint.2018.03.004
7. Haupert, S., Renaud, G., Schumm, A.: Ultrasonic imaging of nonlinear scatterers buried in a medium. NDT E Int. **87**, 1–6 (2017). https://doi.org/10.1016/j.ndteint.2016.12.010
8. Bazulin, E.G.: Decreasing the structural-noise level when performing ultrasonic testing using antenna arrays. Russ. J. Nondestruct. Test. **51**(9), 525–539 (2015). https://doi.org/10.1134/S106183091509003X
9. Bazulin, E.G.: Determination of the reflector type from an image reconstructed using echo signals measured with ultrasonic antenna arrays. Russ. J. Nondestruct. Test. **50**(3), 141–149 (2014). https://doi.org/10.1134/S1061830914030036
10. Bazulin, A.E., Bazulin, E.G., Ismailov, G.M.: The calculation of DGS diagrams for ultrasound testing systems with the use of phased arrays. Russ. J. Nondestruct. Test. **50**(1), 29–37 (2014). https://doi.org/10.1134/S1061830914010033
11. Shah, P.N., White, A., Hensley, D., Papamoschou, D., Vold, H.: Continuous-scan phased array measurement methods for turbofan engine acoustic testing. J. Eng. Gas Turbines Power **141**(8), 081201 (2019). https://doi.org/10.1115/1.4042395
12. Dupont-Marillia, F., Jahazi, M., Lafreniere, S., Belanger, P.: Design and optimisation of a phased array transducer for ultrasonic inspection of large forged steel ingots. NDT E Int. **103**, 119–129 (2019). https://doi.org/10.1016/j.ndteint.2019.02.007
13. Moreau, L., Hunter, A.J., Drinkwater, B.W., Wilcox, P.D.: Efficient imaging techniques using an ultrasonic array. Proc SPIE Int. Soc. Opt. Eng. **7650**, 765037 (2010). https://doi.org/10.1117/12.847294
14. Soldatov, A.I., et al.: Dynamic imaging acoustic fields in research practice. In: Proceedings of the 7th International Forum on Strategic Technology (IFOST 2012), pp. 1–4 (2012). https://doi.org/10.1109/IFOST.2012.6357734
15. Soldatov, A. A., Soldatov, P. V., Soldatov, A. I., Kostina, M. A., Shul'gina, Y. V.: Small-angle acoustic tomography under shadow testing with antenna arrays. Russ. J. Nondestruct. Test. **54**(7), 463–468 (2018). https://doi.org/10.1134/S106183091807007
16. Soldatov, A.I., Kozhemyak, O.A., Soldatov, A.A., Shulgina, Y.V.: Measurement error reducing in the ultrasound time-pulse systems. IOP Conf. Ser. Mater. Sci. Eng. **81**(1), 012117 (2015). https://doi.org/10.1088/1757-899X/81/1/012117
17. Asochakov, A. S., Shulgina, Y. V., Soldatov, A. I., Shulgin, E. M., Ogorodnikov, D. N.: Method of processing of ultrasonic signal of phased array. In: Proceedings of 2015 International Conference on Mechanical Engineering, Automation and Control Systems (MEACS 2015) 7414874 (2016). https://doi.org/10.1109/MEACS.2015.7414874
18. Davy, M., Minonzio, J.-G., de Rosny, J., Prada, C., Fink, M.: Influence of noise on subwavelength imaging of two close scatterers using time reversal method: theory and experiments. Prog. Electromagn. Res. **98**, 333–358 (2009). https://doi.org/10.2528/PIER09071004
19. Asgedom, E.G., Gelius, L.-J., Austeng, A., Holm, S., Tygel, M.: Time-reversal multiple signal classification in case of noise: a phase-coherent approach. J. Acoust. Soc. Am. **130**(4), 2024–2034 (2011). https://doi.org/10.1121/1.3626526
20. Xiao, G., Xiong, C., Hou, Y.: Analyzing phased arrays with basis functions associated with characteristic modes. PIERS-Toyama 2018-August, pp. 208–212 (2018). https://doi.org/10.23919/PIERS.2018.8598107